Flavored Electroweak Baryogenesis: From the LHCb Experiment to Cosmic Baryon Asymmetry

by

Fu Hong SHIU

A Thesis Submitted to
The Hong Kong University of Science and Technology
in Partial Fulfillment of the Requirements for
the Degree of Master of Philosophy
in Physics

August 2014, Hong Kong

Authorization

I hereby declare that I am the sole author of the thesis.

I authorize The Hong Kong University of Science and Technology to lend this thesis to other institutions or individuals for the purpose of scholarly research.

I further authorize The Hong Kong University of Science and Technology to reproduce the thesis by photocopying or by other means, in total or in part, at the request of other institutions or individuals for the purpose of scholarly research.

Fu Hong SHIU

12 August 2014

Flavored Electroweak Baryogenesis: From the LHCb Experiment to Cosmic Baryon Asymmetry

by

Fu Hong SHIU

This is to certify that I have examined the above MPhil thesis and have found that it is complete and satisfactory in all respects, and that any and all revisions required by the thesis examination committee have been made.

Prof Tao LIU, Thesis Supervisor

Prof Michael S ALTMAN, Head of Department

Department of Physics

12 August 2014

Acknowledgment

I would like to express my deep gratitude to my supervisor, Prof. Tao Liu, who has given me a lot of advice and kind support in my research during two years of my MPhil study. He always tries his best to take care of me no matter how busy he is. I have learnt a lot from him, especially in the area of particle phenomenology and cosmology.

I need to thank my collaborators, Prof. Michael Ramsey-Musolf, who has given me advice on the calculations in my work, and Prof. Jing Shu, who introduced to me a very effective method to evaluate loop diagrams.

I also need to thank the people in the Institute for Advanced Studies, Prof. Henry Tye, who has been teaching me to understand physics in different ways, and Prof. Gary Shiu, who has been willing to discuss his innovative ideas with me on cosmology and particle physics. In addition, I would like to thank the postdoctoral fellows, especially Dr. Jan Hajer, Dr. Daniel Junghans, Dr. Pablo Soler and Dr. Yoske Sumitomo, and postgraduate student, Sam Wong SC, for giving me a lot of help and valuable opinions in different ways.

I would also like to thank the Department of Physics for offering me a part-time instructional assistant job, so that I am able to support my study.

Last but not least, I would like to thank my grandmother, my parents and my brother for their emotional and loving support.

Contents

List of Figures

List of Tables

Flavored Electroweak Baryogenesis: From the LHCb Experiment to Cosmic Baryon Asymmetry

Fu Hong SHIU

Department of Physics

Abstract

Baryogenesis has been a candidate mechanism to explain the observed matter-antimatter asymmetry in the Universe ever since Sakharov conditions were proposed in 1967. In order to implement this mechanism, a sizable CP-violating source is needed, which is known to be absent in the Standard Model (SM). Therefore, physics beyond the SM is required to solve this cosmic puzzle. In the context of electroweak baryogenesis (EWBG), flavor-diagonal CP phases are often considered to be such a source, which, however, have been strongly constrained by the null results in Electric Dipole Moment (EDM) measurements. In this work, we propose a new possibility where the EWBG is driven by flavor off-diagonal CP phases. The contribution of such a CP phase to EDM is generically suppressed. Therefore, its magnitude is much less constrained by EDM measurements. As an illustration, we work in the Two Higgs Doublet Model (Type III) and show how flavor off-diagonal CP phases drive the generation of the cosmic baryon asymmetry. Given that searching for flavor off-diagonal CP phases is one of the top-priorities of B physics experiments like LHCb, this study provides a strong theoretical motivation for such measurements.

Chapter 1

Introduction

In this chapter, we review the background of baryon asymmetry of our universe, electroweak baryogenesis and the motivation of our work respectively. In section 1, we discuss the current status of baryon asymmetry of our universe and the necessary conditions for a mechanism to generate baryon asymmetry. In section 2, we give a brief introduction to electroweak baryogenesis and the challenges in standard model. In section 3 and 4, we review the relevant background on electric dipole moment and B physics experiment respectively, which motivate our work.

1.1 Baryon Asymmetry of our Universe

Baryon asymmetry is an obvious fact that our universe is having more matter than antimatter. Naively, if the universe had baryon symmetry, then as the universe has been cooling down, the particle would have annihilated with its anti-particle, the nucleon like proton and neutron do not exist, and there would be no life and hence no human civilization because of the lack of the necessary atoms like hydrogen and helium. Based on this argument, we can reach a conclusion that there must be some asymmetry between matter and anti-matter.

The argument is concrete in the context of Big-Bang Nucleosynthesis, which

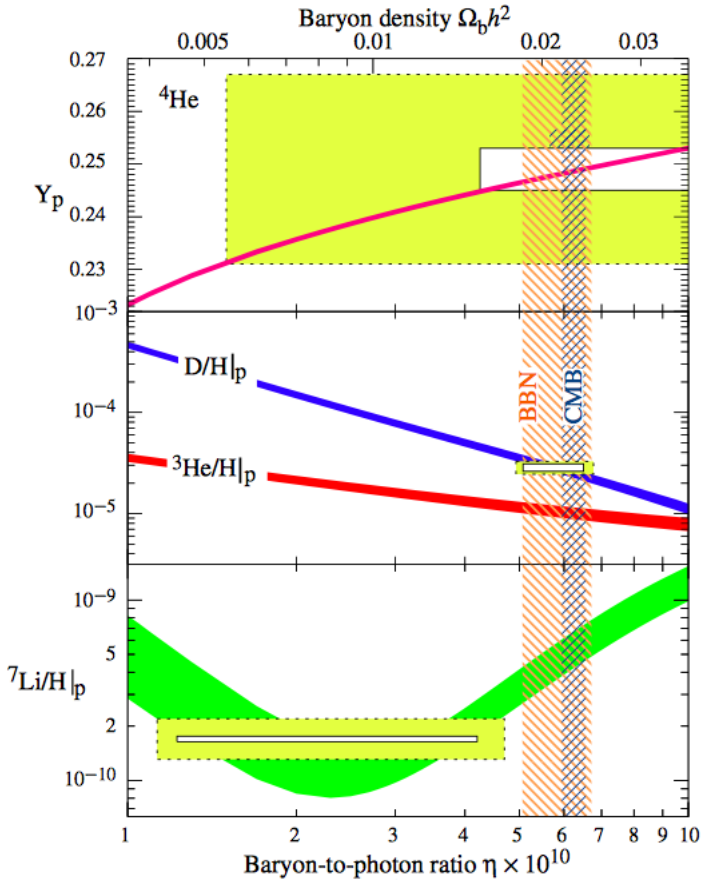

Figure 1.1: The abundances of ^{4}He, D, ^{3}He and ^{7}Li from the prediction of the standard model of Big-Bang Nucleosynthesis, with the bands showing the 95% C.L. range. The observed light element abundances are indicated by the boxes with 95% C.L. range. The orange vertical band indicates the allow range of baryon-to-photon ratio in the context of BBN at 95% C.L. [1]

predicts the abundances of light element isotopes like D, ^{3}He, ^{4}He and ^{7}Li, by only one input parameter baryon-to-photon ratio, η. With the observed abundances, one can trace back the allowed value of η (Fig. 1.1) [1]

$$5.1 \times 10^{-10} \leq \eta \leq 6.5 \times 10^{-10} \quad (95\% \text{ C.L.}) \tag{1.1}$$

or, equivalently, the ratio of net baryon number n_B to entropy s,

$$7.40 \times 10^{-11} \leq \frac{n_B}{s} \leq 9.35 \times 10^{-11} \quad (95\% \text{ C.L.}) \tag{1.2}$$

The non-zero net baryon number followed from eq. (1.2) indicates the baryon

asymmetry of our universe.

1.1.1 Sakharov conditions

In order to explain the baryon asymmetry, Andrei Sakharov proposed in 1967 three necessary conditions for a mechanism (and the underlying theory behind) that is responsible for baryon asymmetry generation [2]:

Baryon number violation

The mechanism must include at least one baryon number violating process like

$$\bar{q}_1 \rightarrow q_2 + q_3 + l$$

where q_i and $\bar{q}_i$ are denoting quark with baryon number $\frac{1}{3}$ and anti-quark with baryon number $-\frac{1}{3}$ respectively; l is denoting lepton which carry zero baryon number. This is an obvious requirement because, otherwise, the present baryon asymmetry can only follow from the initial condition.

C and CP violation

C and CP symmetry are the symmetry between particles and anti-particles. The difference between C and CP is illustrated in Fig. 1.2. The C symmetry is symmetry between $q^{(L)}$ and $\bar{q}^{(L)}$ (as well as $q^{(R)}$ and $\bar{q}^{(R)}$) while CP symmetry is symmetry between $q^{(L)}$ and $\bar{q}^{(R)}$ (as well as $q^{(R)}$ and $\bar{q}^{(L)}$), but both of them imply the symmetry between $q = q^{(L)} + q^{(R)}$ and $\bar{q} = \bar{q}^{(L)} + \bar{q}^{(R)}$. Therefore, if C or CP are the symmetry in the underlying theory, the particles will have identical behavior as anti-particles, then the baryon number density, n_b, should equal to the anti-baryon number density $n_{\bar{b}}$.

One can use the following example to illustrate this idea [3]. Suppose we have three quarks, q_1, q_2, q_3, and one lepton, l, all possible decay modes of the quark q_1 and the corresponding anti-quark $\bar{q}_1$ are listed in Table 1.1. Imagine now we have a box which contains equal amount of q_1 and $\bar{q}_1$. The net baryon number

$$\begin{array}{ccc} q^{(L)} & \xrightarrow{P} & q^{(R)} \\ {\scriptstyle C}\downarrow & \overset{CP}{\searrow} & \downarrow{\scriptstyle C} \\ \bar{q}^{(L)} & \xrightarrow{P} & \bar{q}^{(R)} \end{array}$$

Figure 1.2: The C, P and CP transformation between different components of particle q. (L) and (R) denote the left- and right-handed component respectively.

Process	Branching Ratio	Baryon number
$q_1 \longrightarrow \bar{q}_2\bar{q}_3\bar{l}$	r	$-2/3$
$q_1 \longrightarrow q_2 l\bar{l}$	$1-r$	$1/3$
$\bar{q}_1 \longrightarrow q_2 q_3 l$	$\bar{r}$	$2/3$
$\bar{q}_1 \longrightarrow \bar{q}_2 l\bar{l}$	$1-\bar{r}$	$-1/3$

Table 1.1: Final states and branching ratios for q_1 and $\bar{q}_1$ decay [3]

is hence zero at the beginning, the expected net baryon number after the decay of all the q_1 and $\bar{q}_1$ will be

$$-\frac{2}{3}r + \frac{1}{3}(1-r) + \frac{2}{3}\bar{r} - \frac{1}{3}(1-\bar{r}) = -(r-\bar{r}) \tag{1.3}$$

CP symmetry, as well as C symmetry, implies the equality of the branching ratio, $r = \bar{r}$, and hence the vanishing baryon number at the end. Therefore, one can see that, if nature adores C or CP symmetry, even though the baryon number violating process is present, the net baryon number is still zero.

Departure from thermal equilibrium

There must have been an era in which the particle soup was out of thermal equilibrium. Otherwise, different particle species would have been sharing the same temperature T since the beginning of our universe. The baryon number density, n_b, and anti-baryon number density, $n_{\bar{b}}$, would respectively follow the

distribution function,

$$n_b \propto \int \frac{d^3p}{(2\pi)^3} \frac{1}{\exp\left(\frac{E-\mu_b}{T}\right)+1} \quad \text{and} \quad n_{\bar{b}} \propto \int \frac{d^3p}{(2\pi)^3} \frac{1}{\exp\left(\frac{E+\mu_b}{T}\right)+1} \tag{1.4}$$

where $E = \sqrt{p^2+m_b^2} = \sqrt{p^2+m_{\bar{b}}^2}$ is guaranteed by CPT symmetry. The net baryon number density is given by,

$$n_B = n_b - n_{\bar{b}} \propto T^3 \left[\pi^2 \left(\frac{\mu_b}{T}\right) + \left(\frac{\mu_b}{T}\right)^3\right] \tag{1.5}$$

The chemical equilibrium implies the vanishing baryon chemical potential, $\mu_b = 0$. The net baryon number density would have kept zero through out the evolution of our universe.

1.2 Electroweak Baryogenesis as a Baryon Generating Mechanism

Electroweak baryogenesis (EWBG) [4, 5, 6] is a mechanism to produce the net baryon number during electroweak phase transition (EWPT). When the universe was cooling down, due to the Hubble expansion, to the electroweak scale, $T \approx 100$ GeV, the Higgs field obtains a non-zero vacuum expectation value (vev) which spontaneously breaks the electroweak symmetry $\mathrm{SU}(2)_L \otimes \mathrm{U}(1)_Y$ to $\mathrm{U}(1)_{\mathrm{EM}}$, and gives masses to the particles such as quarks and leptons. In this subsection, we will see how Sakharov conditions in the EWBG are satisfied.

1.2.1 B violating process: Weak sphaleron process

In the standard model (SM), the baryon and lepton numbers are conserved at the classical level, but at the loop level, an anomaly exists,

$$\partial_\mu J^\mu_{\mathrm{B+L}} = \frac{3}{16\pi^2}\left[g^2 \mathrm{Tr}\left(F_{\mu\nu}\tilde{F}^{\mu\nu}\right) - g'^2 B_{\mu\nu}\tilde{B}^{\mu\nu}\right] \tag{1.6}$$

$$\partial_\mu J^\mu_{\mathrm{B-L}} = 0 \tag{1.7}$$

where $F_{\mu\nu}$ and $B_{\mu\nu}$ are the $\mathrm{SU}(2)_L$ and $\mathrm{U}(1)_Y$ field strength respectively, and g and g' are the corresponding gauge couplings. These equations mean that the fluctuation of the gauge fields can induce fluctuation and hence the non-conservation of baryon (B) and lepton (L) number, even though the difference $\mathrm{B}-\mathrm{L}$ is conserved. The change of the total baryon number from time t_i to t_f is

$$B(t_f) - B(t_i) = 3\left[N_{CS}(t_f) - N_{CS}(t_i)\right] \tag{1.8}$$

where N_{CS} is the Chern-Simons number. This number is used to classify the time-independent vacuum solutions to the electroweak field equations, that is, minima of the electroweak potential energy. Therefore, different solutions correspond to the configuration with different baryon and lepton numbers. It has been discussed in [7, 8] that energy barrier exists between the minima, so that the field fluctuating around the potential minimum cannot change their vacuum state easily. At high energy, the field needs not to sit at the minima. The field sitting at the top of the barrier is called sphaleron, which has potential energy proportional to the Higgs vev [7, 8]

$$E_{\mathrm{sph}} = B \cdot \frac{2M_W}{\alpha_w} \propto \phi_0 \tag{1.9}$$

where M_W is the W boson mass, α_w is the weak coupling and B is a constant which can be evaluated numerically. In the SM, $1.5 \leq B \leq 2.7$ [9]. Since sphalerons are the solutions that correspond to the top of the energy barriers, they are unstable. They can cross the barriers passing through the minima with different Chern-Simons number, and hence cause baryon violation. This process is called sphaleron process.

The sphaleron process in weak sector (weak sphaleron) is an ingredient in the SM. Therefore, to implement the B violating process, we do not need any physics beyond the SM. As it is the process in weak sector, only left-handed particles or right-handed antiparticles get involved. Whenever the process is active, it can convert baryons to antileptons and antibaryons, or antibaryons to leptons and baryons. At finite temperature, the weak sphaleron interaction rate depends on

whether the electroweak symmetry is broken. In the broken phase, the rate is exponentially [10, 11] suppressed

$$\Gamma_{ws} \propto \exp\left(-\frac{E_{\rm sph}}{T}\right) \propto \exp\left(-\frac{\phi_0\left(T\right)}{T}\right) \tag{1.10}$$

while in the symmetric phase, [12]

$$\Gamma_{ws} = \kappa\alpha_w^5 T \tag{1.11}$$

where $\kappa \approx 120$. The feature that the weak sphaleron is active before but is suppressed after EWPT allows us to involve this B violating process into the scenario of EWBG, which happened during EWPT.

1.2.2 C/CP violating interaction

In the SM, only left-handed particles and right-handed antiparticles get involved into weak interaction, the C symmetry is hence violated maximally. However, for the CP violation, there is only one flavor off-diagonal CP phase showing up in the interactions between W boson and quarks (CKM CP phase), the CP violation due to this phase is not directly related to EWBG, which, as we shall discuss, requires the CP violation in the interactions between Higgs boson and particles. Therefore, it is not surprised that the baryon asymmetry sourced by this CP phase in the context of EWBG is of the order [13],

$$\left|\frac{n_B}{s}\right| \sim 10^{-27} \tag{1.12}$$

which is negligible compared to eq. (1.2).

1.2.3 Departure of thermal equilibrium: First order phase transition

If there is a barrier for Higgs field to gain the non-zero vev, the electroweak symmetry will be broken locally instead of globally and simultaneously. This

will lead to the formation of bubbles. The region inside the bubbles has the phase that the electroweak symmetry is broken; while the region outside has the phase that the symmetry is still preserved. At a sufficiently low temperature, the nucleated bubbles with an initial large enough size keep expanding; the bubbles finally collide and combine to make the whole universe being in the broken phase [14]. This transition is of first-order phase transition.

The picture can be described by finite-temperature quantum field theory. At the non-zero temperature, the Higgs potential suffers from thermal correction. At high temperature, the effective potential, e.g. in the SM, can be approximated by [15, 16]

$$V_{\text{eff}}(\phi, T) \approx D \cdot \left(T^2 - T_0^2\right) |\phi|^2 - E \cdot T^3 |\phi|^3 + \lambda |\phi|^4 \tag{1.13}$$

where D, E and λ are slowly varying positive functions of time. T_0 is some temperature at which the second derivative of the potential at $\phi = 0$ is zero, the transition after which is no longer of first order because the remaining symmetric phase is transiting to the broken phase without bubble nucleation. Non-zero E in eq. (1.13) indicates the existence of a barrier in the potential. In this case, the second minimum $\langle\phi\rangle = \phi_c$ degenerated to $\langle\phi\rangle = 0$ appears at a certain temperature, which is defined to be critical temperature T_c and can be expressed in terms of the parameters in the potential,

$$\frac{\phi_c}{T_c} = \frac{E}{2\lambda} \tag{1.14}$$

At the temperature around or below the critical temperature, $T \lesssim T_c$, the Higgs field $\phi(x)$ tunneling through the barrier will cause a bubble nucleating at the region around x. This is the key feature of first order phase transition.

In EWBG, the net baryon number density, n_B, is determined by [17]

$$\dot{n}_B \simeq -\Gamma_{\text{ws}} n_B \tag{1.15}$$

where the weak sphaleron rate $\Gamma_{\text{ws}} \propto \exp(-\phi_0/T)$ in the broken phase as we have discussed. The net baryon number density inside the bubble at time t is

hence roughly,

$$n_B(t) \sim n_B(T_c) \cdot \exp\left[-\exp\left(-\frac{\phi_c}{T_c}\right)\right] \tag{1.16}$$

Therefore, a successful EWBG requires a strong first order phase transition, eq. (1.17), to avoid the net baryon being washed out in the bubble wall [17],

$$\frac{\phi_c}{T_c} \gtrsim 1 \tag{1.17}$$

1.2.4 Baryon creation in electroweak baryogenesis

If all of the conditions above are satisfied, then the baryon asymmetry can be generated via four steps [14, 18]:

1. Higgs nucleation bubbles are formed due to the strong first order phase transition.

2. The particles in the symmetric phase scatter with the bubble walls. The CP violating interactions generate the number density difference between left-handed particles and right-handed antiparticles in front of the wall.

3. The particle soup with this asymmetry diffuses. The weak sphaleron process active in symmetric phase converts the particle number asymmetry into baryon asymmetry.

4. The expanding bubble wall captures the baryon asymmetry. As the weak sphaleron transition is highly suppressed in the broken phase, the baryon number is basically frozen inside the bubble wall until today.

1.2.5 Challenges

As we have seen in the last subsection, the number asymmetry of left-handed particles, which bias the weak sphaleron process generating net baryon number, is produced by the CP violating interactions between particles and bubble wall that is classical profile of Higgs field. Therefore, in order to generate baryon

asymmetry through EWBG, CP phases have to be introduced into Higgs couplings. However, as we have discussed in section 1.2.2, in the SM, there is only one CP phase and it is installed into the couplings between W boson and fermions instead of Higgs couplings. This CP phase can only contribute to the baryon asymmetry beyond the classical level. Also, the Jarlskog invariant, which is a rephasing invariant measure of CP violation, is too small for this CP phase [52].

$$J_{\rm CP}^{(\rm SM)} = (2.96 \pm 0.20) \times 10^{-5} \tag{1.18}$$

Therefore, the baryon asymmetry due to this CP phase is negligible.

To generate enough baryon asymmetry generated via EWBG, we need CP phases beyond the SM. There has been a lot of experimental searches for the new CP phases, but in most of the theoretical studies, only flavor diagonal CP phases are considered as the source to EWBG [19, 20, 21, 22]. However, we will see in the next section that flavor diagonal CP phases in Higgs couplings are strongly constrained by electric dipole moment measurements, so it would be a challenge to use them to drive EWBG.

1.3 Electric Dipole Moment

In this section, we review the relevant background on electric dipole moment [23, 24, 25], and use the measurement of electron electric dipole moment as an example to illustrate how the flavor diagonal CP phases as the source of EWBG, are challenged by the null result of electric dipole moment measurements.

Consider a system, in which there could be elementary particles, nucleon or atom. Under a weak external electric field $\vec{E}$, the energy shift of the system due to the electric field is

$$H = -p_i E_i - p_{ij} E_i E_j + \dots \tag{1.19}$$

the vector quantity $\vec{p}$ is the electric dipole moment (EDM) of the system, and is defining how the system responds the external electric field linearly. The

relativistic generalization of the first term in eq. (1.19) for spin-1/2 particles, denoted by the Dirac spinor ψ, is

$$\mathcal{L}_{\rm EDM} = -d \cdot \frac{i}{2} \bar{\psi} \sigma^{\mu\nu} \gamma_5 \psi F_{\mu\nu} \tag{1.20}$$

where $\sigma^{\mu\nu} = \frac{i}{2}[\gamma^\mu, \gamma^\nu]$ and $F_{\mu\nu}$ is the electromagnetic field strength. In the non-relativistic limit, eq. (1.20) reduces to

$$\mathcal{L}_{\rm EDM} \to d \cdot \chi^\dagger \sigma_i \chi E_i = d\vec{S} \cdot \vec{E} \tag{1.21}$$

The EDM of the elementary particles is generally proportional to their spin, the proportionality constant d, which is in the unit of e cm, hence determines how large the EDM is. The operator eq. (1.20) violates CP (and P), therefore, the non-zero d must be induced by the CP phases in the underlying theory.

1.3.1 Electron EDM

In the SM, the electron EDM first appears at four-loop order and the numerical estimated of the electron EDM due to the CKM CP phase are of the order [26],

$$\left|d_e^{\rm CKM}\right| \lesssim 10^{-37} e \text{ cm} \tag{1.22}$$

while the current experimental upper bound with 90% C.L. [27] is

$$|d_e| < 8.7 \times 10^{-29} e \text{ cm} \tag{1.23}$$

which is compatible with the SM prediction.

In physics beyond the SM, the leading order contribution could come from two loops due to non-standard Higgses as shown in Fig. (1.3). In the figure, the CP phase is introduced in the Higgs-top-top coupling, and hence it is a flavor diagonal CP phase and is related to EWBG as well. However, as demonstrated by [25], the electron EDM gets contributed by these "Barr-Zee" type diagrams, and it put strong bounds on the flavor diagonal CP phases used for EWBG.

For flavor off-diagonal CP phases, their contribution to EDM are generically small. In two loops diagrams, e.g. Fig. (1.4), the contribution is zero due to a

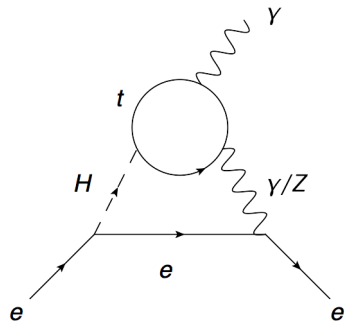

Figure 1.3: An example of two-loop contribution ("Barr-Zee" type diagram) to the electron EDM. H denotes the non-standard Higgs boson, flavor diagonal CP phase shows up in the Htt vertex.

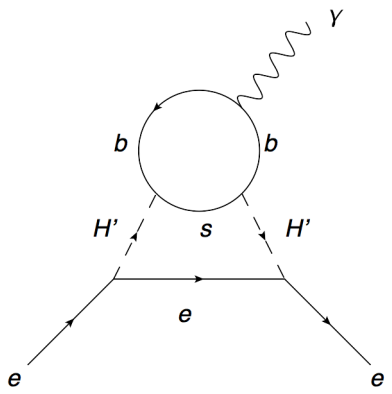

Figure 1.4: An example of possible two-loop contribution to the electron EDM. H' denotes the non-standard Higgs boson that is responsible for flavor changing neutral process, flavor off-diagonal CP phases show up in the $H'bs$ vertex.

cancellation of CP phases along the fermion loop. So the flavor off-diagonal CP phases are much less constrained by the EDM measurements, and leave a room for us to explore the possibility that they can drive the EWBG.

1.4 B Physics

Another motivation on our exploration is B physics experiments like the LHCb. In this section, we review the aim of LHCb experiment and the background of one of their measurements, $B_s^0 - \bar{B}_s^0$ mixing, which will be used to bound the CP violation parameters in our later discussion.

1.4.1 LHCb experiment

The LHCb (Large Hardon Collider beauty) experiment is one of the four Large Hardon Collider (LHC) experiments at CERN. It aims at exploring physics after the Big Bang to see how nature prefers matter over anti-matter, by recording the decay of B mesons, which contains bottom or anti-bottom quark.

The source of b hadrons comes from the LHC. In proton-proton collisions at center-of-mass energy $\sqrt{s} = 14$ TeV, the $b\bar{b}$ production cross section is expected to be $\sim 500\mu$b and is dominated by the gluon fusion. At the nominal LHC, the luminosity is designed to be $10^{10}\text{b}^{-1}\text{sec}^{-1}$, while the luminosity at LHCb is relatively low, whose mean value is within $2 - 5 \times 10^{8}\text{b}^{-1}\text{sec}^{-1}$ for technical reasons [28]. The measurements in LHCb includes $B_s^0 \to \mu\mu$, $B_d^0 \to K^*\mu\mu$, $K_s^0 \to \mu\mu$ decays, and B_s^0, B_d^0 and D oscillations. The results will allow us to place the constraints on the parameters related to flavor physics, especially the flavor off-diagonal CP phases.

1.4.2 $B_s^0 - \bar{B}_s^0$ mixing

In this subsection, we briefly introduce the mixing and decay of the B_s^0 or $\bar{B}_s^0$ mesons. The evolution of the B_s^0 meson system can be generally described by

the quantum state [29],

$$|\psi(t)\rangle = \psi_1(t)\left|B_s^0\right\rangle + \psi_2(t)\left|\bar{B}_s^0\right\rangle + a(t)|n_1\rangle + b(t)|n_2\rangle + c(t)|n_3\rangle + \ldots \quad (1.24)$$

where $|B_s^0\rangle$ and $\left|\bar{B}_s^0\right\rangle$ are the CP eigenstates of the B_s^0 system, $|n_1\rangle$, $|n_2\rangle$ and $|n_3\rangle$ are some states describing the B_s^0 decay products. As ψ_1 and ψ_2 already contain sufficient information about the $B_s^0 - \bar{B}_s^0$ mixing and decay, we will adopt the Wigner-Weisskopf approximation [29, 30] and focus on the observables related to these quantity at the meson rest frame. The evolution of

$$|\psi(t)\rangle = \psi_1(t)\left|B_s^0\right\rangle + \psi_2(t)\left|\bar{B}_s^0\right\rangle \quad (1.25)$$

satisfies the Schrodinger equation,

$$i\frac{d}{dt}\begin{pmatrix}\psi_1\\ \psi_2\end{pmatrix} = H\begin{pmatrix}\psi_1\\ \psi_2\end{pmatrix} = \begin{pmatrix}R_{11} & R_{12}\\ R_{21} & R_{22}\end{pmatrix}\begin{pmatrix}\psi_1\\ \psi_2\end{pmatrix} \quad (1.26)$$

Here the matrix R here is not Hermitian because the meson could decay, with

$$R = M + \frac{i}{2}\Gamma \quad (1.27)$$

where M and Γ are Hermitian matrix. In terms of the Hamiltonian of underlying theory H,

$$M_{ij} = \langle i|H|j\rangle \quad (1.28)$$

$$\Gamma_{ij} = 2\pi\sum_f \delta(E_n - \bar{m})\langle i|H|f\rangle\langle f|H|j\rangle \quad (1.29)$$

The CPT invariance of the SM implies that $M_{11} = M_{22}$ and $\Gamma_{11} = \Gamma_{22}$. On the other hand, eq. (1.27) admits two eigenvalues that are generally complex,

$$\mu_H = m_H + \frac{i}{2}\Gamma_H \quad (1.30)$$

$$\mu_L = m_L + \frac{i}{2}\Gamma_L \quad (1.31)$$

We can then define

$$\bar{m} = \frac{m_H + m_L}{2} \tag{1.32}$$

$$\bar{\Gamma} = \frac{\Gamma_H + \Gamma_L}{2} \tag{1.33}$$

$$\Delta m = m_H - m_L \tag{1.34}$$

$$\Delta\Gamma = \Gamma_H - \Gamma_L \tag{1.35}$$

in which m is the mass and Γ is the decay width of the meson, H and L are standing for heavy and light eigenstate respectively. The non-zero R_{12} and R_{21} mean that the mass eigenstates can never simultantaneously be the CP eigenstates. Therefore, the observed B_s^0 meson could oscillate between B_s^0 and $\bar{B}_s^0$ before it decays, this phenomenon is known as $B_s^0 - \bar{B}_s^0$ mixing.

Chapter 2

From Flavor Off-diagonal CP violation to Electroweak Baryogenesis

In Chapter 1, we see that the cosmic baryon asymmetry relies on the CP asymmetry involved in the interactions between particles and Higgs field. The CP phase in SM does not work because the Jarlskog invariant is small. Therefore, we need to seek for physics beyond the SM in which new CP phases are introduced. In our work, we consider type III Two Higgs Doublet Model. By adding one more Higgs doublet and extending the Yukawa sector, one can introduce flavor off-diagonal CP phases into the couplings between fermions and non-standard Higgses, and implement the EWBG.

In this chapter, in section 1, we give a brief introduction to type III Two Higgs Doublet Model and clarify the phenomenological simplification we use for the remaining analysis. In section 2, based on the reasonable assumptions, we introduce diffusion equations and discuss the dependence of baryon asymmetry on flavor off-diagonal CP phases.

2.1 Two Higgs Doublet Model

In the general context of Two Higgs Doublet Model (2HDM) subject to $\mathrm{SU}(2)_L \otimes \mathrm{U}(1)_Y$, the Higgs sector contains two $\mathrm{SU}(2)_L$ doublet Φ_1 and Φ_2 with hypercharge Y_1 and Y_2 respectively. By convention, the doublet Φ_1 acquires the vacuum expectation value (vev) of the form,

$$\langle \Phi_1 \rangle = \frac{1}{\sqrt{2}} \begin{pmatrix} 0 \\ v_1 \end{pmatrix} \quad \text{and} \quad Y_1 = \frac{1}{2} \tag{2.1}$$

If the model is to be broken into $\mathrm{U}(1)_{\mathrm{EM}}$, then the vev of the doublet Φ_2 must have the form,

$$\langle \Phi_2 \rangle = \frac{1}{\sqrt{2}} \begin{pmatrix} 0 \\ v_2 \end{pmatrix} \quad \text{and} \quad \text{if } Y_2 = \frac{1}{2} \tag{2.2}$$

or

$$\langle \Phi_2 \rangle = \frac{1}{\sqrt{2}} \begin{pmatrix} v_2 \\ 0 \end{pmatrix} \quad \text{and} \quad \text{if } Y_2 = -\frac{1}{2} \tag{2.3}$$

where $v_2 = |v_2| e^{i\theta_2}$ may carry a non-zero phase in general. But by re-defining $\Phi_2 \rightarrow e^{-i\theta_2}\Phi_2$, the phase can be absorbed into the coefficients in the Higgs potential and the Yukawa sector.

In what following, we consider $Y_1 = Y_2 = \frac{1}{2}$ and define

$$\langle \Phi_1 \rangle = \frac{1}{\sqrt{2}} \begin{pmatrix} 0 \\ v_1 \end{pmatrix} = \frac{1}{\sqrt{2}} \begin{pmatrix} 0 \\ v\cos\beta \end{pmatrix} \tag{2.4}$$

$$\langle \Phi_2 \rangle = \frac{1}{\sqrt{2}} \begin{pmatrix} 0 \\ v_2 \end{pmatrix} = \frac{1}{\sqrt{2}} \begin{pmatrix} 0 \\ v\sin\beta \end{pmatrix} \tag{2.5}$$

where $v = \sqrt{v_1^2 + v_2^2}$ and $\tan\beta = v_2/v_1$.

2.1.1 Yukawa sector

The 2HDM is often into 3 types. Depending on the symmetry inserting on the fields, the Yukawa sector is different in these 3 types [46]:

Type I: Discrete symmetry $\Phi_2 \to -\Phi_2$

$$\mathcal{L}_{\text{Yukawa, 2HDM-I}} = -\lambda_d^{ij} \bar{Q^i}_L \Phi_1 d_R^j - \lambda_u^{ij} \bar{Q_L^i} \tilde{\Phi}_1 u_R^j + h.c. \tag{2.6}$$

Type II: Discrete symmetry $\Phi_2 \to -\Phi_2$ and $d_R^i \to -d_R^i$

$$\mathcal{L}_{\text{Yukawa, 2HDM-II}} = -\lambda_u^{ij} \bar{Q_L^i} \tilde{\Phi}_1 u_R^j - y_d^{ij} \bar{Q^i}_L \Phi_2 d_R^j + h.c. \tag{2.7}$$

Type III: No Discrete symmetry

$$\begin{aligned} \mathcal{L}_{\text{Yukawa, 2HDM-III}} = & -\lambda_d^{ij} \bar{Q^i}_L \Phi_1 d_R^j - \lambda_u^{ij} \bar{Q_L^i} \tilde{\Phi}_1 u_R^j \\ & -y_d^{ij} \bar{Q^i}_L \Phi_2 d_R^j - y_u^{ij} \bar{Q_L^i} \tilde{\Phi}_2 u_R^j + h.c. \end{aligned} \tag{2.8}$$

where $i, j = 1, 2, 3$ stands respectively for three familiars.

$$Q_L^i = \begin{pmatrix} u_L^i \\ d_L^i \end{pmatrix} = \left(\begin{pmatrix} u_L \\ d_L \end{pmatrix}, \begin{pmatrix} c_L \\ s_L \end{pmatrix}, \begin{pmatrix} t_L \\ b_L \end{pmatrix} \right) \tag{2.9}$$

$$u_R^i = (u_R, c_R, t_R) \quad \text{and} \quad d_R^i = (d_R, s_R, b_R) \tag{2.10}$$

In type I model, the up-type and down-type quark mass matrix are proportional to λ_u and λ_d respectively; while in type II model, they are proportional to λ_u and y_d respectively. By diagonalizing the mass matrices and expressing the quark fields in term of their mass eigenstate, one can see that the FCNP mediated by non-standard neutral Higgs bosons at tree level is absent in both type I and type II model.

In type III model, the Yukawa sector takes on the most general gauge invariant form. If we work in the Higgs basis $\{H_1, H_2\}$ [29],

$$\begin{bmatrix} H_1 \\ H_2 \end{bmatrix} = \begin{bmatrix} \cos\beta & \sin\beta \\ -\sin\beta & \cos\beta \end{bmatrix} \begin{bmatrix} \Phi_1 \\ \Phi_2 \end{bmatrix} \tag{2.11}$$

so that the vev appears only in the doublet H_1,

$$\begin{aligned} H_1 &= \begin{bmatrix} G^+ \\ \frac{1}{\sqrt{2}}(v+h_1)+\frac{i}{\sqrt{2}}G^0 \end{bmatrix} \\ H_2 &= \begin{bmatrix} H^+ \\ \frac{1}{\sqrt{2}}h_2+\frac{i}{\sqrt{2}}A \end{bmatrix} \end{aligned} \tag{2.12}$$

eq. (2.8) becomes [29]

$$\begin{aligned} \mathcal{L}_{\text{Yukawa}} &= -\left(1+\frac{h_1}{v}\right)\left(\bar{u}_L M_u u_R + \bar{d}_L M_d d_R\right) \\ &\quad -\frac{\sqrt{2}}{v}\cdot\frac{h_2+iA}{\sqrt{2}}\left(\bar{d}_L Y_d d_R - \bar{u}_R Y_u^\dagger u_L\right) - \frac{\sqrt{2}}{v}H^+\left(\bar{u}_L Y_d d_R - \bar{u}_R Y_u^\dagger d_L\right) \\ &\quad -\frac{\sqrt{2}}{v}G^+\left(\bar{u}_L M_d d_R - \bar{u}_R M_u^\dagger d_L\right) - i\cdot\frac{G^0}{v}\left(\bar{d}_L M_d d_R - \bar{u}_L M_u u_R\right) \\ &\quad +h.c. \end{aligned} \tag{2.13}$$

with $M = \frac{\lambda v\cdot\cos\beta + yv\cdot\sin\beta}{\sqrt{2}}$ being the quark mass matrix and $Y = \frac{-\lambda v\cdot\sin\beta + yv\cdot\cos\beta}{\sqrt{2}}$.

By expressing the quark fields in term of their mass eigenstate under unitary weak-basis-transformation, i.e. $q_L \to U_{q_L} q_L$ and $q_R \to U_{q_R} q_R$,

$$\begin{aligned} \mathcal{L}_{\text{Yukawa}} &= -\left(1+\frac{h_1}{v}\right)\left(\sum_{u,c,t} m_u \bar{u}_L u_R + \sum_{d,s,b} m_d \bar{d}_L d_R\right) \\ &\quad -\frac{\sqrt{2}}{v}\cdot\frac{h_2+iA}{\sqrt{2}}\left(\bar{d}_L N_D d_R - \bar{u}_R N_U^\dagger u_L\right) \\ &\quad -\frac{\sqrt{2}}{v}H^+\left[\bar{u}_L\left(V N_D\right)d_R - \bar{u}_R\left(N_U^\dagger V\right)d_L\right] \\ &\quad -\frac{\sqrt{2}}{v}G^+\left[\bar{u}\left(m_d V P_R - m_u V P_L\right)d\right] - i\cdot\frac{G^0}{v}\left(m_d\bar{d}_L d_R - m_u\bar{u}_L u_R\right) \\ &\quad +h.c. \end{aligned} \tag{2.14}$$

where

$$N_U = U_{u_L}^\dagger Y_u U_{u_R} \tag{2.15}$$

$$N_D = U_{d_L}^\dagger Y_d U_{d_R} \tag{2.16}$$

are completely arbitrary [46]. Their matrix elements can be complex number, which introduce new CP-phases. They are not necessarily diagonal, and hence introduce a CP-violating flavor-changing neutral process (FCNP) at tree level, mediated by the linear combination of neutral Higgs mass eigenstates $(h_2+iA)/\sqrt{2}$.

2.1.2 Phenomenological Simplification

Without the loss of generality, we assume in our work that the yukawa coupling for the down type quark sector having the following form

$$\lambda = \sqrt{2}\begin{bmatrix} 0 & 0 & 0 \\ 0 & \pm\xi_{ss} & 0 \\ 0 & \xi_{bs}e^{i\theta_{\lambda_{bs}}} & \pm\xi_{bb} \end{bmatrix} \quad \text{and} \quad y = \sqrt{2}\begin{bmatrix} 0 & 0 & 0 \\ 0 & \pm\xi_{ss} & 0 \\ 0 & \pm\xi_{bs} & \pm\xi_{bb} \end{bmatrix} \tag{2.17}$$

where the ξ_{ij} are all positive and real. The phase $\theta_{\lambda_{bs}}$ is an irreducible phase after the appropriate field redefinition. We shall assume another physical phase comes from the up-sector yukawa coupling, which exists in the CKM matrix and do not contribute to our following discussion. We will see that, in the massless limit of s quark, $\theta_{\lambda_{bs}}$ sources both cosmic baryon asymmetry and B meson CP-violating observables. The mass matrix in $b-s$ sector is then [31]

$$M_d = \begin{bmatrix} \pm 2\xi_{ss} & 0 \\ \xi_{bs}\left(\pm 1 + e^{i\theta_{\lambda_{bs}}}\right) & \pm 2\xi_{bb} \end{bmatrix} v \tag{2.18}$$

The mass matrix can be diagonalized as eq. (2.14) with the bottom quark mass, in terms of ξ and $\theta_{\lambda_{bs}}$, given by

$$m_b = 2v \cdot \sqrt{\xi_{bb}^2 + \xi_{bs}^2 \cos^2\frac{\theta_{\lambda_{bs}}}{2}} \quad \text{or} \quad 2v \cdot \sqrt{\xi_{bb}^2 + \xi_{bs}^2 \sin^2\frac{\theta_{\lambda_{bs}}}{2}} \tag{2.19}$$

for $y_{bs} > 0$ and < 0 respectively. U_{d_L} is an identity matrix and U_{d_R} can be parametrized by a rotation angle α, so that

$$U_{d_R} = \begin{bmatrix} \cos\alpha & -e^{\frac{-i\theta_{\lambda_{bs}}}{2}}\sin\alpha \\ e^{\frac{i\theta_{\lambda_{bs}}}{2}}\sin\alpha & \cos\alpha \end{bmatrix} \tag{2.20}$$

with

$$\tan\alpha = \frac{\xi_{bs}\left|\cos\frac{\theta_{\lambda_{bs}}}{2}\right|}{\xi_{bb}} \quad \text{or} \quad \frac{\xi_{bs}\left|\sin\frac{\theta_{\lambda_{bs}}}{2}\right|}{\xi_{bb}} \tag{2.21}$$

The corresponding eq. (2.16) gives,

$$N_D = \begin{bmatrix} 0 & 0 \\ \left(\mp 1 + e^{i\theta_{\lambda_{bs}}}\right)\xi_{bs}\cos\alpha & \mp 2i\frac{\xi_{bs}^2\sin\theta_{\lambda_{bs}}}{m_b} \end{bmatrix} v \tag{2.22}$$

The physical phase $\theta_{\lambda_{bs}}$ controls the strength of flavor off-diagonal CP violation. In the next section, we will discuss how this CP phase enters the calculation of EWBG and affects the generation of the cosmic baryon asymmetry.

2.2 Boltzmann equations

As mentioned in chapter 1, EWBG consists of several processes including scattering and diffusion in the vicinity of expanding bubble walls. The presence of C and CP violating interactions ensures the generation of particle number asymmetry, that will then bias the weak sphaleron process to generate more baryon than anti-baryon.

2.2.1 CP violating interaction at the boundary

At the first stage, we write down a set of coupled differential equations for various particle densities through the effect of diffusion, particle number changing interactions and CP violating source terms. We aim at extracting the information the net number density of all left-handed quarks, which would then convert to the net baryon number through the weak sphaleron process at the second stage.

Defining H, Q_i, $U_i = \{U, C, T\}$, $D_i = \{D, S, B\}$ to be respectively the number density of Higgs boson, left-handed quarks, right-handed up-type quarks, and right-handed down-type quarks of three different families, $i = 1, 2, 3$. The interactions between the particles were dominated by top yukawa (with rate Γ_t), top relaxation processes (with rate Γ_{m_t}), Higgs relaxation processes (with rate Γ_h) and strong sphaleron processes, whose interaction rate at temperature T is $\Gamma_{ss} = 16\alpha_s^4 T$ [14], where α_s is the strong coupling constant. First, the light quarks, such as up quark, down quark and charm quark, are mainly produced by strong sphaleron processes. Second, all quarks have similar diffusion constants. Third, at this step, the processes taken into account conserve baryon number on the time-scales shorter than the inverse electroweak sphaleron rate,

$\Gamma_{ws} \approx 120\alpha_w^5 T$ [14]. These facts imply that [31]

$$Q_1 = -2U = -2D = -2C = -2B \tag{2.23}$$

$$S + T + Q_3 = 0 \tag{2.24}$$

The Boltzmann equations that govern the interaction between the particles and the bubble boundary are [31]

$$\begin{aligned}
\dot{Q}_3 &= D_q \nabla^2 Q_3 + \Gamma_{m_t}(\xi_T - \xi_{Q_3}) + \Gamma_t(\xi_T - \xi_{Q_3} - \xi_H) \\
&\quad + 2\Gamma_{ss}\left(\xi_T - 2\xi_{Q_3} + \xi_S + 8\xi_B\right) + S_{b_L}^{CP} \qquad (2.25) \\
\dot{T} &= D_q \nabla^2 T - \Gamma_{m_t}(\xi_T - \xi_{Q_3}) - \Gamma_t\left(\xi_T - \xi_H - \xi_{Q_3}\right) \\
&\quad - \Gamma_{ss}\left(\xi_T - 2\xi_{Q_3} + \xi_S + 8\xi_B\right) \qquad (2.26) \\
\dot{H} &= D_h \nabla^2 H + \Gamma_t\left(\xi_T - \xi_H - \xi_{Q_3}\right) - 2\Gamma_h H \qquad (2.27) \\
\dot{S} &= D_q \nabla^2 S - \Gamma_{ss}\delta_{ss} + S_{s_R}^{CP} \qquad (2.28) \\
\dot{B} &= D_q \nabla^2 B - \Gamma_{ss}\delta_{ss} \qquad (2.29)
\end{aligned}$$

where D_i is a diffusion constant and $\xi_i = \frac{n_i}{k_i}$ with n_i being the number density and k_i being a statistical factor of particle species i. The CP violating process $b_L \to s_R$ mediated by non-standard Higgs bosons contributes as a source term, $S_{b_L}^{CP} = -S_{s_R}^{CP}$, which will be discussed in section 1.2.3. To simplify the discussion, we work at the local rest frame of the bubble wall by $r - v_w t = \bar{z}$, and hence neglect the wall curvature.

$$\left(\partial_t, \nabla^2\right) \to \left(-v_w \partial_{\bar{z}}, \partial_{\bar{z}}^2\right)$$

where v_w is the wall expanding speed measured at the rest frame of the bubble center, $\bar{z} > 0$ corresponds to the symmetric phase while $\bar{z} < 0$ corresponds to the broken phase. Assuming the CP violating source term vanishing inside bubbles, $S_{b_L}^{CP}\left(\bar{z} < 0\right) = 0$, we solve the set of eq. (2.25-2.29) at the leading order in $\frac{1}{\Gamma_{ss}}$, it yields the approximate result of the number density of left-handed quarks $n_L = \sum_{i=1}^{3} Q_i$ in the symmetric phase,

$$n_L\left(\bar{z} > 0\right) = -\frac{3k_R}{14k_H}\frac{v_w^2}{\Gamma_{ss}\bar{D}}\left(1 - \frac{D_q}{\bar{D}}\right)\frac{\bar{S}\left(\bar{z}\right)}{\kappa^+} \tag{2.30}$$

with

$$\kappa^{\pm} = \frac{v_w \pm \sqrt{v_w^2 + 4\bar{D}\bar{\Gamma}}}{2\bar{D}} \tag{2.31}$$

$$\bar{D} = \frac{7D_h k_H + 6D_q k_R}{7k_H + 6k_R} \tag{2.32}$$

$$\bar{\Gamma} = \frac{7\left(2\Gamma_h + \Gamma_{m_t}\right)}{7k_H + 6k_R} \tag{2.33}$$

$$\bar{S} = -\frac{k_H S_{b_L}^{CP}}{7k_H + 6k_R} \tag{2.34}$$

in which we have assumed $2k_R = k_{Q_3} = 2k_T = 2k_B = 2k_S$.

2.2.2 Weak sphaleron process

At the second stage, the weak sphaleron process, which happens at the longer time scale $\Gamma_{ws} \approx 120\alpha_w^5 T$ in the symmetric phase, converts the generated left-handed quarks number density, eq. (2.30), into baryon asymmetry ρ_B, which is described by [32],

$$\partial_\mu \rho_B^\mu = -\Theta\left(-\bar{z}\right)\Gamma_{ws}\left(\frac{15}{4}\rho_B + 3n_L\right) \tag{2.35}$$

Here, we assume the weak sphaleron rate is negligible inside the broken phase due to the exponential suppression. The net baryon number density in the broken phase is hence a constant [31]

$$\rho_B\left(\bar{z} < 0\right) = \frac{3\Gamma_{ws}}{\Gamma_{ss}}\left[-\frac{3k_R}{14k_H}\frac{v_w^2}{\bar{D}}\left(1 - \frac{D_q}{\bar{D}}\right)\right]\int_0^\infty \frac{\bar{S}\left(\bar{z}\right)}{\kappa^+} e^{-\kappa^+ \bar{z}} d\bar{z} \tag{2.36}$$

2.2.3 CP violation source

The CP violating source term in the Boltzmann equations is induced by the CP violating transition, $b_L \to s_R$ which is mediated by non-standard Higgs bosons. In the previous work [31], the source term has been computed using closed time path formulation. The result is

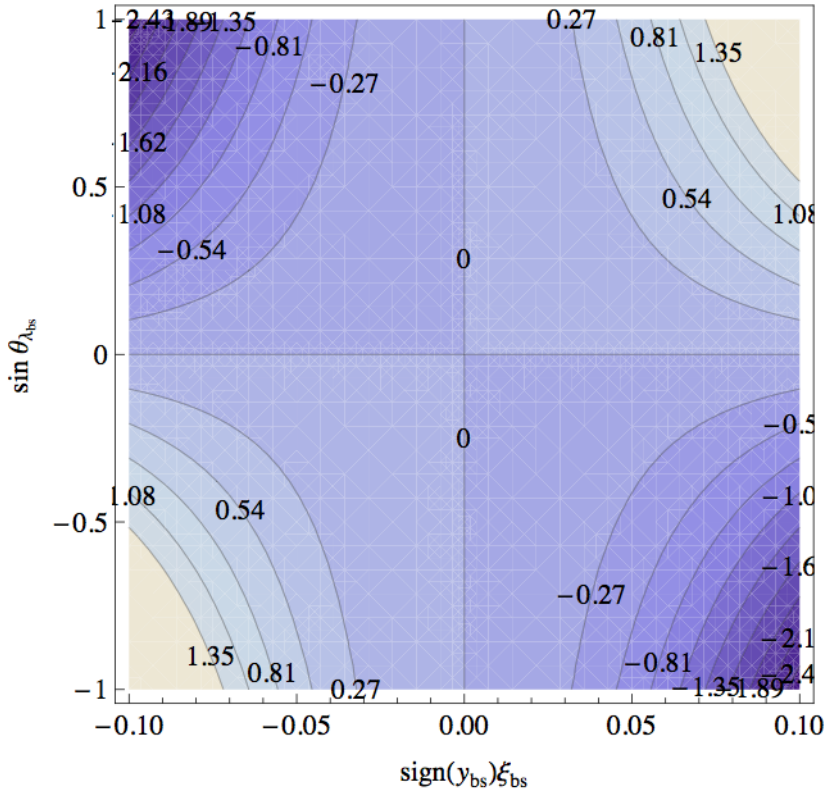

Figure 2.1: Contours of $\frac{n_B}{s}$ (in units of 10^{-10}) under the assumption $k_R = 3$[33], $k_H = 4$, $v_w = 0.4$[34], $D_q = \frac{6}{T}$ and $D_h = \frac{110}{T}$.

$$S_{b_L}^{CP} = \frac{N_c \left|M_{bs}\left(\bar{z}\right)\right|^2}{\pi^2} \frac{\partial \theta_{bs}\left(\bar{z}\right)}{\partial \bar{z}} \int_0^\infty \frac{k^2 dk}{\omega_{b_L} \omega_{s_R}} \operatorname{Im}\left\{ \frac{\left(\epsilon_{b_L}^* \epsilon_{s_R} - k^2\right)\left[n_F\left(\epsilon_{s_R}\right) - n_F\left(\epsilon_{b_L}^*\right)\right]}{\left(\epsilon_{s_R} - \epsilon_{b_L}^*\right)^2} + \frac{\left(\epsilon_{b_L} \epsilon_{s_R} + k^2\right)\left[n_F\left(\epsilon_{s_R}\right) + n_F\left(\epsilon_{b_L}^*\right)\right]}{\left(\epsilon_{s_R} + \epsilon_{b_L}\right)^2} \right\} \tag{2.37}$$

where n_F is the Fermi distribution, $\epsilon_i = \omega_i - i\Gamma_i$ and $\omega_i^2 = k^2 + m_i^2$ in which Γ_i and m_i are thermal parameters corresponding to different particle species i. The flavor off-diagonal CP phase introduced in eq. (2.17) enters the source term by the quantity $\frac{\partial \theta_{bs}(\bar{z})}{\partial \bar{z}}$, which is given by

$$\frac{\partial \theta_{bs}\left(\bar{z}\right)}{\partial \bar{z}} = -\frac{f\left(\bar{z}\right)}{\left|M_{bs}\left(\bar{z}\right)\right|^2} \cdot \operatorname{sign}\left(y_{bs}\right) \xi_{bs}^2 \sin\theta_{\lambda_{bs}} \tag{2.38}$$

with $f\left(\bar{z}\right)$ being a function describing the Higgs vev profile across the bubble wall.

By taking a global view on eqs. (2.36,2.37,2.38), we can see that the net baryon density frozen in the broken phase is proportional to the flavor off-diagonal CP phase [31]

$$\rho_B\left(\bar{z} < 0\right) \propto \int_0^\infty f\left(\bar{z}\right) \operatorname{sign}\left(y_{bs}\right) \xi_{bs}^2 \sin\theta_{\lambda_{bs}} d\bar{z} \tag{2.39}$$

The concrete dependence of the baryon asymmetry on the Yukawa parameters ξ_{bs} and $\theta_{\lambda_{bs}}$ is shown in Fig. (2.1). To see whether the flavor off-diagonal CP phase can contribute a non-negligible cosmic baryon asymmetry, we need to look for experimental bounds on these parameters. As we have discussed in section 2.1, apart from CP violating interaction at bubble walls, the parameters ξ_{bs} and $\theta_{\lambda_{bs}}$ are responsible for the flavor changing neutral process in $b - s$ sector too. Provided that searching for the CP phase in this process is one of the top priorities of B physics experiments, in the next chapter, we will use the B physics experimental results to constrain the parameters ξ_{bs} and $\theta_{\lambda_{bs}}$, and see how much baryon asymmetry can be generated by using flavor off-diagonal CP phase.

Chapter 3

Experimental Measurements

In this chapter, we work on the implications of the flavor off-diagonal CP phase for $B_s^0 - \bar{B}_s^0$ mixing and $\bar{B} \to X_s\gamma$, through flavor transition mediated by non-standard Higgs bosons. By employing the present experimental results from LHCb, we put the constraints on the yukawa parameter ξ_{bs} and the off-diagonal CP phase $\theta_{\lambda_{bs}}$.

3.1 $B_s^0 - \bar{B}_s^0$ mixing

3.1.1 Contribution from 2HDM-III

Unlike the SM, the leading order contribution to the $B_s^0 - \bar{B}_s^0$ mixing comes from the tree level non-standard neutral Higgses (CP-even and CP-odd) exchange. If we assume the two non-standard Higgs bosons have the same mass 500 GeV for simplicity, the amplitude is

$$\frac{4G_F}{\sqrt{2}}\frac{i}{m_h^2}\left[\left(N_{D,bs}\right)^2 \bar{b}P_R s \cdot \bar{b}P_R s + \left(N_{D,sb}^*\right)^2 \bar{b}P_L s \cdot \bar{b}P_L s\right] \tag{3.1}$$

where $m_h = 500$ GeV is the mass of both two non-standard neutral Higgs boson.

On the other hand, the effective weak Hamiltonian describing the $B_s^0 - \bar{B}_s^0$ mixing reads [53]

$$H_{\text{eff}}^{\Delta B=2} = \frac{4G_F}{\sqrt{2}}\sum_i C_i\left(\mu\right) Q_i\left(\mu\right) \tag{3.2}$$

where $C_i(\mu)$ are scale-dependent Wilson coefficients and Q_i are the relevant $\Delta B = 2$ operators, given by

$$\begin{aligned}
Q_1^{\mathrm{VLL}} &= \left(\bar{b}\gamma_\mu P_L s\right)\left(\bar{b}\gamma^\mu P_L s\right) \\
Q_1^{\mathrm{VRR}} &= \left(\bar{b}\gamma_\mu P_R s\right)\left(\bar{b}\gamma^\mu P_R s\right) \\
Q_1^{\mathrm{LR}} &= \left(\bar{b}\gamma_\mu P_L s\right)\left(\bar{b}\gamma^\mu P_R s\right) \\
Q_2^{\mathrm{LR}} &= \left(\bar{b}P_L s\right)\left(\bar{b}P_R s\right) \\
Q_1^{\mathrm{SLL}} &= \left(\bar{b}P_L s\right)\left(\bar{b}P_L s\right) \\
Q_2^{\mathrm{SLL}} &= \left(\bar{b}\sigma_{\mu\nu} P_L s\right)\left(\bar{b}\sigma^{\mu\nu} P_L s\right) \\
Q_1^{\mathrm{SRR}} &= \left(\bar{b}P_R s\right)\left(\bar{b}P_R s\right) \\
Q_2^{\mathrm{SRR}} &= \left(\bar{b}\sigma_{\mu\nu} P_R s\right)\left(\bar{b}\sigma^{\mu\nu} P_R s\right)
\end{aligned} \tag{3.3}$$

with $\sigma_{\mu\nu} = \frac{1}{2}\left[\gamma_\mu, \gamma_\nu\right]$ and $P_{L,R} = \frac{1}{2}\left(1 \mp \gamma_5\right)$. Since QCD preserves chirality, there is no mixing between different sector (VLL, VRR, LR, SLL, SRR) during the RG-running due to $\alpha_s(\mu)$.

By matching eq. (3.1) and eq. (3.2), the Wilson coefficients at Higgs mass scale μ_h are summarized as,

$$C_1^{\mathrm{VLL}} = C_1^{\mathrm{VRR}} = 0 \tag{3.4}$$

$$C_1^{\mathrm{LR}}(\mu_H) = C_2^{\mathrm{LR}} = C_2^{\mathrm{SLL}}(\mu_H) = C_2^{\mathrm{SRR}}(\mu_H) = 0 \tag{3.5}$$

$$C_1^{\mathrm{SLL}}(\mu_H) = \left(\frac{(N_D)_{bs}}{m_h}\right)^2 \tag{3.6}$$

$$C_1^{\mathrm{SRR}}(\mu_H) = \left(\frac{(N_D)^*_{sb}}{m_h}\right)^2 \tag{3.7}$$

Under the renormalization group (RG) running, the operators eq. (3.3) can mix.

The non-zero Wilson coefficients at the lower energy scale μ_t are,

$$\begin{aligned} C_1^{\mathrm{SLL/SRR}}(\mu_t) &= \big(1.0743\eta_6^{-0.6916} - 0.0631\eta_6^{0.3084} \\ &\quad -0.0119\eta_6^{0.7869} + 0.0006\eta_6^{1.7869}\big)\, C_1^{\mathrm{SLL/SRR}}(\mu_H) \end{aligned} \tag{3.8}$$

$$\begin{aligned} C_2^{\mathrm{SLL/SRR}}(\mu_t) &= \big(-0.0076\eta_6^{-0.6916} - 0.0005\eta_6^{0.3084} \\ &\quad +0.0075\eta_6^{0.7869} - 0.0003\eta_6^{1.7869}\big)\, C_1^{\mathrm{SLL/SRR}}(\mu_H) \end{aligned} \tag{3.9}$$

where the number of active quarks is $f = 6$ during the running from $\mu = \mu_h$ to μ_t, and hence we use,

$$\eta_6 = \left.\frac{\alpha_s(\mu_H)}{\alpha_s(\mu_t)}\right|_{f=6} \tag{3.10}$$

The matrix element $\left\langle \bar{B}_s^0 \left| H_{\mathrm{eff}} \right| B_s^0 \right\rangle$, in terms of the B_s meson m_{B_s}, decay constant F_{B_s} and the Wilson coefficients, can be written as follows [53]

$$\begin{aligned} \left\langle \bar{B}_s^0 \left| \mathcal{H}_{\mathrm{eff}}^{\Delta B=2} \right| B_s^0 \right\rangle &= \frac{4G_F}{\sqrt{2}} \cdot \frac{1}{3} m_{B_s} F_{B_s}^2 \, \{ \\ &\quad P_1^{\mathrm{VLL}} \left[C_1^{\mathrm{VLL}}(\mu_t) + C_2^{\mathrm{VLL}}(\mu_t) \right] \\ &\quad + P_1^{\mathrm{LR}} C_1^{\mathrm{LR}}(\mu_t) + P_2^{\mathrm{LR}} C_2^{\mathrm{LR}}(\mu_t) \\ &\quad + P_1^{\mathrm{SLL}} \left[C_1^{\mathrm{SLL}}(\mu_t) + C_1^{\mathrm{SRR}}(\mu_t) \right] \\ &\quad + P_2^{\mathrm{SLL}} \left[C_2^{\mathrm{SLL}}(\mu_t) + C_2^{\mathrm{SRR}}(\mu_t) \right] \} \end{aligned} \tag{3.11}$$

with

$$P_1^{\mathrm{VLL}} = 0.84 \tag{3.12}$$

$$P_1^{\mathrm{LR}} = 1.62, \; P_2^{\mathrm{LR}} = 2.46 \tag{3.13}$$

$$P_1^{\mathrm{SLL}} = -1.47, \; P_2^{\mathrm{SLL}} = -2.98 \tag{3.14}$$

3.1.2 Experimental Bound

As mentioned in chapter 1, the evolution of the B_s^0 system is controlled by $M_{12}^s = \left\langle \bar{B}_s^0 \left| \mathcal{H}_{\mathrm{eff}}^{\Delta B=2} \right| B_s^0 \right\rangle$. Refer to the parameterization in [36], $M_{12}^s = \left(M_{12}^s\right)^{\mathrm{SM}} \Delta_s$ with

Theoretical input	
$\Delta m_s^{\rm SM}$	19.30 ± 2.2 ps^{-1}
$\Delta\Gamma_s^{\rm SM}$	0.098 ± 0.024 ps^{-1}
$\phi_s^{\rm SM}$	$(4.2 \pm 1.4) \times 10^{-3}$
F_{B_s}	238.8 ± 9.5 MeV
Experimental data	**LHCb**
Δm_s	17.725 ± 0.049 ps^{-1}
$\Delta\Gamma_s$	0.123 ± 0.030 ps^{-1}

Table 3.1: The theoretical input parameters [1, 37, 38] and the experimental data from the LHCb.

$\Delta_s = |\Delta_s|\, e^{i\phi_s^\Delta}$, the mass and decay width difference between the heavy and light B_s mass eigenstates, Δm_s and $\Delta\Gamma_s$, are generally expressed by

$$\begin{aligned} \Delta m_s &= \Delta m_s^{\rm SM}\, |\Delta_s| \\ \Delta\Gamma_s &= \Delta\Gamma_s^{\rm SM} \cos\left(\phi_s^{\rm SM} + \phi_s^\Delta\right) \end{aligned} \tag{3.15}$$

The theoretical and experimental information are shown in 3.1. Assuming the mass of the non-standard Higgs bosons, $m_h = 500$ GeV, we perform the χ^2 fitting to the observables in eq. (3.15). We scan over the Yukawa parameters ξ_{bs} and $\sin\theta_{\lambda_{bs}}$, yielding the regions of 95% confidence level from the LHCb results (Fig. 3.1).

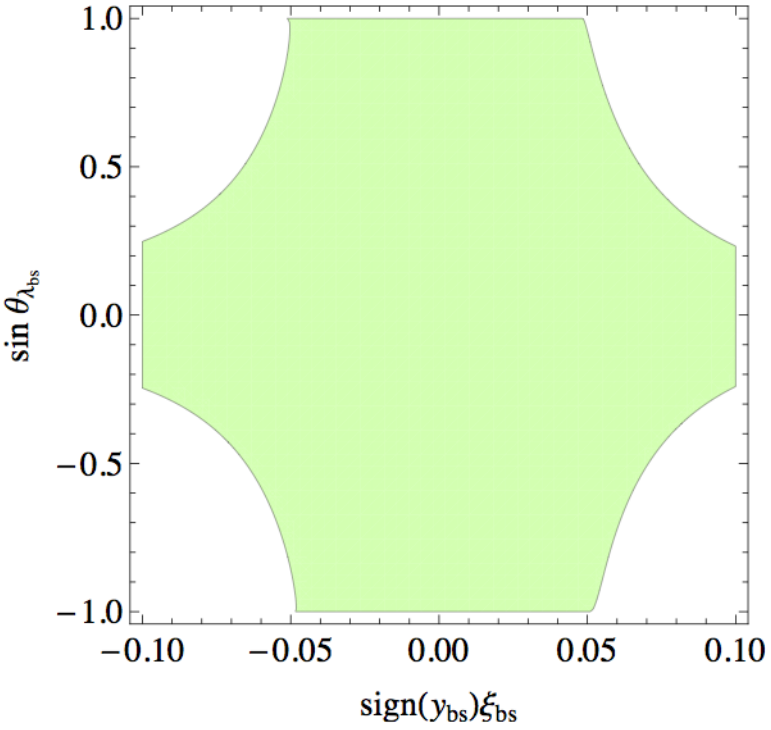

Figure 3.1: $B_s^0 - \bar{B}_s^0$ mixing: Green contours indicate 95% C.L. LHCb constraints under the assumption that the mass of non-standard Higgs bosons is 500 GeV.

3.2 $\bar{B} \to X_s\gamma$

3.2.1 Contribution in 2HDM-III

The effective weak Hamiltonian for $\bar{B} \to X_s\gamma$ reads [53]

$$H_{\text{eff}}^{\Delta F=2} = \frac{4G_F}{\sqrt{2}} \cdot V_{st}^{\dagger} V_{tb} \cdot \sum_i \left[C_i^{(L)}(\mu)\, O_i^{(L)}(\mu) + C_i^{(R)}(\mu)\, O_i^{(R)}(\mu) \right] \tag{3.16}$$

Apart from those in the SM,

$$
\begin{aligned}
O_1^{(L)} &= (\bar{s}_i\gamma^\mu P_L c_j)\,(\bar{c}_j\gamma_\mu P_L b_i) \\
O_2^{(L)} &= (\bar{s}\gamma^\mu P_L c)\,(\bar{c}\gamma_\mu P_L b) \\
O_3^{(L)} &= (\bar{s}\gamma^\mu P_L b)\,(\bar{q}\gamma_\mu P_L q) \\
O_4^{(L)} &= (\bar{s}_i\gamma^\mu P_L b_j)\,(\bar{q}_j\gamma_\mu P_L q_i) \\
O_5^{(L)} &= (\bar{s}\gamma^\mu P_L b)\,(\bar{q}\gamma_\mu P_R q) \\
O_6^{(L)} &= (\bar{s}_i\gamma^\mu P_L b_j)\,(\bar{q}_j\gamma_\mu P_R q_i)
\end{aligned}
$$

$$
\begin{aligned}
O_{7\gamma}^{(R)} &= \frac{e}{16\pi^2} m_b \cdot \bar{s}\sigma^{\mu\nu} P_R b \cdot F_{\mu\nu} \\
O_{8g}^{(R)} &= \frac{g_s}{16\pi^2} m_b \cdot \bar{s}_i\sigma^{\mu\nu} P_R T^a_{ij} b_j \cdot G^a_{\mu\nu}
\end{aligned}
\tag{3.17}
$$

we will have the opposite-parity counterpart,

$$
\begin{aligned}
O_1^{(R)} &= (\bar{s}_i\gamma^\mu P_R c_j)\,(\bar{c}_j\gamma_\mu P_R b_i) \\
O_2^{(R)} &= (\bar{s}\gamma^\mu P_R c)\,(\bar{c}\gamma_\mu P_R b) \\
O_3^{(R)} &= (\bar{s}\gamma^\mu P_R b)\,(\bar{q}\gamma_\mu P_R q) \\
O_4^{(R)} &= (\bar{s}_i\gamma^\mu P_R b_j)\,(\bar{q}_j\gamma_\mu P_R q_i) \\
O_5^{(R)} &= (\bar{s}\gamma^\mu P_R b)\,(\bar{q}\gamma_\mu P_L q) \\
O_6^{(R)} &= (\bar{s}_i\gamma^\mu P_R b_j)\,(\bar{q}_j\gamma_\mu P_L q_i)
\end{aligned}
$$

$$
\begin{aligned}
O_{7\gamma}^{(L)} &= \frac{e}{16\pi^2} m_b \cdot \bar{s}\sigma^{\mu\nu} P_L b \cdot F_{\mu\nu} \\
O_{8g}^{(L)} &= \frac{g_s}{16\pi^2} m_b \cdot \bar{s}_i\sigma^{\mu\nu} P_L T^a_{ij} b_j \cdot G^a_{\mu\nu}
\end{aligned}
\tag{3.18}
$$

By matching the amplitude from eq. (3.2) with the effective Hamiltonian, the leading order Wilson coefficients contributed by the 2HDM-III at the energy

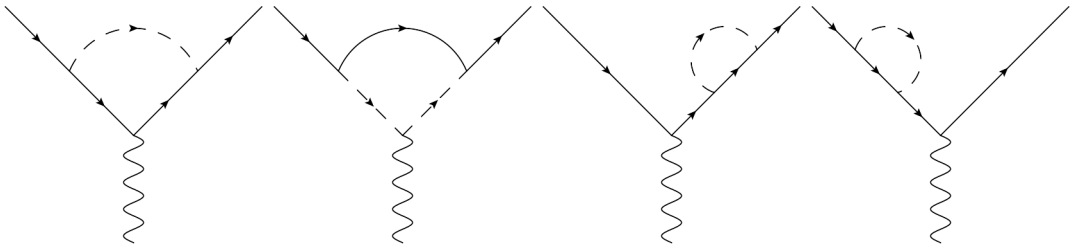

Figure 3.2: All the topologies (a) - (d) getting involved in charged higgs contribution to $b \to s\gamma$, while only (a), (b), (d) getting involved in $b \to sg$ and non-standard neutral higgs contribution to $b \to s\gamma$

scale μ_H are given by

$$\begin{aligned} C_{7\gamma,\mathrm{NP}}^{(L)(0)}(\mu_H) &= \sum_{q=u,c,t}\left[\frac{\left(N_D^\dagger V^\dagger\right)_{sq}(VN_D)_{qb}}{3m_q^2}F_7^{(1)}\left(x_q^{H^\pm}\right) - \frac{\left(N_D^\dagger V^\dagger\right)_{sq}(VN_D)_{qb}}{m_q m_b}F_7^{(2)}\left(x_q^{H^\pm}\right)\right] \\ &\quad -\frac{1}{6}\sum_{q=d,s,b}\left[\frac{\left(N_D^\dagger\right)_{sq}(N_D)_{qb}}{3m_q^2}\left(F_8^{(1)}\left(x_q^{h_2}\right)+F_8^{(1)}\left(x_q^{A}\right)\right)\right] \\ &\quad -\frac{1}{6}\sum_{q=d,s,b}\left[\frac{\left(N_D^\dagger\right)_{sq}(N_D)_{qb}}{m_q m_b}\left(F_8^{(2)}\left(x_q^{h_2}\right)-F_8^{(2)}\left(x_q^{A}\right)\right)\right] \end{aligned} \tag{3.19}$$

$$\begin{aligned} C_{7\gamma,\mathrm{NP}}^{(R)(0)}(\mu_H) &= \sum_{q=u,c,t}\left[\frac{\left(V^\dagger N_U\right)_{sq}\left(N_U^\dagger V\right)_{qb}}{3m_q^2}F_7^{(1)}\left(x_q^{H^\pm}\right) - \frac{\left(V^\dagger N_U\right)_{sq}(VN_U)_{qb}}{m_q m_b}F_7^{(2)}\left(x_q^{H^\pm}\right)\right] \\ &\quad -\frac{1}{6}\sum_{q=d,s,b}\left[\frac{\left(N_D^\dagger\right)_{sq}(N_D)_{qb}}{3m_q^2}\left(F_8^{(1)}\left(x_q^{h_2}\right)+F_8^{(1)}\left(x_q^{A}\right)\right)\right] \\ &\quad -\frac{1}{6}\sum_{q=d,s,b}\left[\frac{(N_D)_{sq}(N_D)_{qb}}{m_q m_b}\left(F_8^{(2)}\left(x_q^{h_2}\right)-F_8^{(2)}\left(x_q^{A}\right)\right)\right] \end{aligned} \tag{3.20}$$

$$\begin{aligned} C_{8g,\mathrm{NP}}^{(L)(0)}(\mu_H) &= \sum_{q=u,c,t}\left[\frac{\left(N_D^\dagger V^\dagger\right)_{sq}(VN_D)_{qb}}{3m_q^2}F_8^{(1)}\left(x_q^{H^\pm}\right) - \frac{\left(N_D^\dagger V^\dagger\right)_{sq}(VN_D)_{qb}}{m_q m_b}F_8^{(2)}\left(x_q^{H^\pm}\right)\right] \\ &\quad +\frac{1}{2}\sum_{q=d,s,b}\left[\frac{\left(N_D^\dagger\right)_{sq}(N_D)_{qb}}{3m_q^2}\left(F_8^{(1)}\left(x_q^{h_2}\right)+F_8^{(1)}\left(x_q^{A}\right)\right)\right] \\ &\quad +\frac{1}{2}\sum_{q=d,s,b}\left[\frac{\left(N_D^\dagger\right)_{sq}\left(N_D^\dagger\right)_{qb}}{m_q m_b}\left(F_8^{(2)}\left(x_q^{h_2}\right)-F_8^{(2)}\left(x_q^{A}\right)\right)\right] \end{aligned} \tag{3.21}$$

$$
\begin{aligned}
C_{8g,\mathrm{NP}}^{(R)(0)}\left(\mu_H\right) &= \sum_{q=u,c,t}\left[\frac{\left(V^{\dagger}N_U\right)_{sq}\left(N_U^{\dagger}V\right)_{qb}}{3m_q^2}F_8^{(1)}\left(x_q^{H^{\pm}}\right)-\frac{\left(V^{\dagger}N_U\right)_{sq}\left(VN_U\right)_{qb}}{m_q m_b}F_8^{(2)}\left(x_q^{H^{\pm}}\right)\right] \\
&+\frac{1}{2}\sum_{q=d,s,b}\left[\frac{\left(N_D\right)_{sq}\left(N_D^{\dagger}\right)_{qb}}{3m_q^2}\left(F_8^{(1)}\left(x_q^{h_2}\right)+F_8^{(1)}\left(x_q^{A}\right)\right)\right] \\
&+\frac{1}{2}\sum_{q=d,s,b}\left[\frac{\left(N_D\right)_{sq}\left(N_D\right)_{qb}}{m_q m_b}\left(F_8^{(2)}\left(x_q^{h_2}\right)-F_8^{(2)}\left(x_q^{A}\right)\right)\right] \qquad (3.22)
\end{aligned}
$$

where $x_i^f=\frac{m_i^2}{m_f^2}$ and the definition of A_0, F_0, $F_7^{(1)}$, $F_8^{(1)}$, $F_7^{(2)}$ and $F_8^{(2)}$ is given in the Appendix A.

The RG running of $O_{7\gamma}$ and O_{8g} involves a mixture of eq. (3.17-3.18),

$$
\begin{aligned}
C_{7\gamma,\mathrm{NP}}^{(0)}\left(\mu_b\right) &= \eta_5^{\frac{16}{23}}\eta_6^{\frac{16}{21}}C_{7\gamma,\mathrm{NP}}^{(0)}\left(\mu_H\right) \qquad (3.23)\\
&+\frac{8}{3}\left[\eta_6^{\frac{2}{3}}\left(\eta_5^{\frac{14}{23}}-\eta_5^{\frac{16}{23}}\right)+\eta_5^{\frac{16}{23}}\left(\eta_6^{\frac{2}{3}}-\eta_6^{\frac{16}{21}}\right)\right]C_{8g,\mathrm{NP}}^{(0)}\left(\mu_H\right) \\
C_{8g,\mathrm{NP}}^{(0)}\left(\mu_b\right) &= \eta_5^{\frac{14}{23}}\eta_6^{\frac{2}{3}}C_{8g,\mathrm{NP}}^{(0)}\left(\mu_H\right) \qquad (3.24)
\end{aligned}
$$

where

$$
\eta_6=\left.\frac{\alpha_s\left(\mu_H\right)}{\alpha_s\left(\mu_t\right)}\right|_{f=6} \qquad \eta_5=\left.\frac{\alpha_s\left(\mu_t\right)}{\alpha_s\left(\mu_b\right)}\right|_{f=5}
$$

3.2.2 Experimental Bound from the Branching Ratio

In our analysis, the branching ratio of the decay $\bar{B}\to X_s\gamma$ is given by [49, 35, 50, 51],

$$
\mathrm{Br}\left(\bar{B}\to X_s\gamma\right)=\mathrm{Br}_{\mathrm{SM}}^{\mathrm{NNLO}}+0.00247\left[\left|C_{7\gamma,\mathrm{NP}}^{(L)}\left(\mu_b\right)\right|^2+\left|C_{7\gamma,\mathrm{NP}}^{(R)}\left(\mu_b\right)\right|^2-0.706\mathrm{Re}\left(C_{7\gamma,\mathrm{NP}}^{(L)}\left(\mu_b\right)\right)\right] \qquad (3.25)
$$

where $\mathrm{Br}_{\mathrm{SM}}^{\mathrm{NNLO}}=(315\pm23)\times10^{-6}$. Its global average from HFAG [43] is

$$
\mathrm{Br}\left(\bar{B}\to X_s\gamma\right)_{\mathrm{exp}}=(355\pm24\pm9)\times10^{-6} \qquad (3.26)
$$

We preform a Gaussian fit to the branching ratio in eq. (3.25), under the same assumption that all non-standard Higgs boson (both charged and neutral) have the same mass 500 GeV. The allowed region at 95% C.L. is shown in Fig. 3.3.

Fig. (3.3) shows the experimental constraints from the branching ratio of the decay $\bar{B}\to X_s\gamma$. We see that the bound is weak such that the parameter space

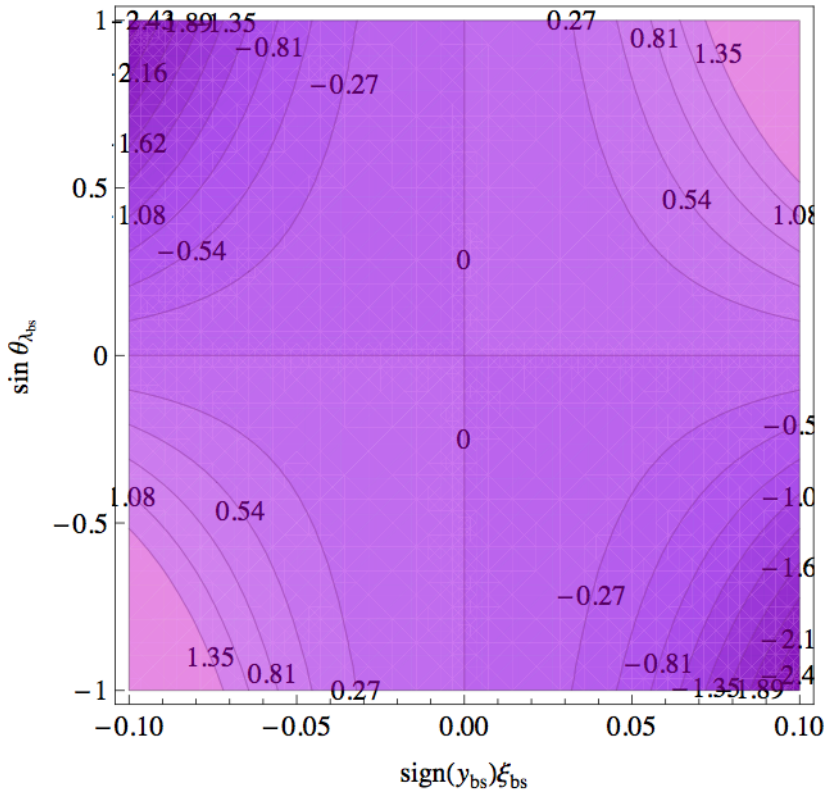

Figure 3.3: $\bar{B} \to X_s\gamma$: Purple contours indicate 95% C.L. experimental constraints under the assumption that the mass of non-standard Higgs bosons is 500 GeV.

showed in Fig. (3.3) is allowed. If we go back to eq. (3.25), when new physics contribution to the Wilson coefficients $|C_{7\gamma,\mathrm{NP}}| \ll 1$, eq. (3.25) is approximately

$$\mathrm{Br}\left(\bar{B} \to X_s\gamma\right) \approx \mathrm{Br}_{\mathrm{SM}}^{\mathrm{NNLO}} - 1.74 \times 10^{-3} \cdot \mathrm{Re}\left(C_{7\gamma,\mathrm{NP}}^{(L)}\left(\mu_b\right)\right) \tag{3.27}$$

According to eq. (3.19), we have

$$C_{7\gamma,\mathrm{NP}}^{(L)} \propto \frac{N_{D,bs}^{*} N_{D,bb}}{m_h^2} \tag{3.28}$$

Since we assume $|\lambda_{bs}| = |y_{bs}| = \xi_{bs}$, it implies $N_{D,bs} \propto \xi_{bs} v$ and $N_{D,bb} \propto \xi_{bs}^2 v$. In the parameter region, $\xi_{bs} < 0.1$, the Wilson coefficient $C_{7\gamma,\mathrm{NP}}$ is of the order $\mathcal{O}\left(10^{-4}\right)$. The new physics contribution to the branching ratio is of the order $\mathcal{O}\left(10^{-7}\right)$, while the SM prediction and the experimental result are both of the order $\mathcal{O}\left(10^{-4}\right)$ with the error of $\mathcal{O}\left(10^{-5}\right)$. So the contribution is negligible. However, we have $|\lambda_{bs}| \neq |y_{bs}|$ in a general case. We expect $N_{D,bs} \sim N_{D,bb} \propto \xi_{bs} v + \mathcal{O}\left(\xi_{bs}^2\right)$ and a stronger bound on ξ_{bs} and $\sin\theta_{\lambda_{bs}}$ from $\mathrm{Br}\left(\bar{B} \to X_s\gamma\right)$.

Chapter 4

Summary and Outlook

The combined plot is shown in Fig. 4.1. Even though the constraints from the observables in $B_s^0 - \bar{B}_s^0$ mixing are much stronger than from Br $\left(\bar{B} \to X_s\gamma\right)$, we can still see that a non-negligible amount of baryon asymmetry can be generated, compared to the full baryon asymmetry $0.74 \times 10^{-10} \leq \frac{n_B}{s} \leq 0.94 \times 10^{-10}$.

It is worth to note that the bounds in the plot depend also on the mass of the non-standard Higgs bosons. The new physics contribution is smaller when the non-standard Higgs bosons are heavier. Therefore, a larger range for ξ_{bs} and $\sin\theta_{bs}$, and hence a larger cosmic baryon asymmetry are allowed if we increase the mass of non-standard Higgs bosons. However, one should also note that the parameter ξ_{bs} cannot be arbitrarily large, otherwise, the mass of the bottom quark, which is around 5 GeV, cannot be recovered. A combination of these constraints will necessarily provide definite information on the non-standard Higgs bosons as well as the flavored EWBG. We leave the investigation of this regard to a later work.

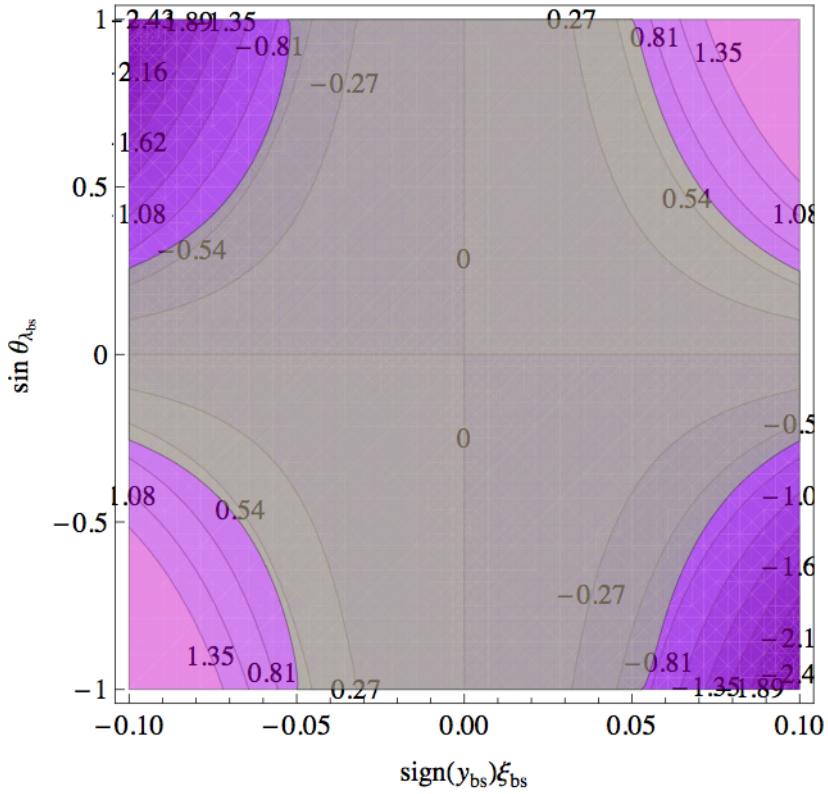

Figure 4.1: Contour of constant $^{n_B}/_s$. Purple and grey colors denote the regions allowed by the measurements of Br $\left(\bar{B} \to X_s\gamma\right)$ and $B_s^0 - \bar{B}_s^0$ mixing, respectively.

Appendix A

Loop Integral Functions

The loop integral functions used above are defined following conventions of the SuperIso package [44]

$$
\begin{aligned}
A_0(x) &= \frac{-3x^3+2x^2}{2(1-x)^4}\ln x + \frac{22x^3-153x^2+159x-46}{36(1-x)^3} \\
F_0(x) &= \frac{3x^2}{2(1-x)^4}\ln x + \frac{5x^3-9x^2+30x-8}{12(1-x)^3} \\
F_7^{(1)}(x) &= \frac{x(7-5x-8x^2)}{24(x-1)^3} + \frac{x^2(3x-2)}{4(x-1)^4}\ln x \\
F_8^{(1)}(x) &= \frac{x(2+5x-x^2)}{8(x-1)^3} - \frac{3x^2}{4(x-1)^4}\ln x \\
F_7^{(2)}(x) &= \frac{x(3-5x)}{12(x-1)^2} - \frac{x(3x-2)}{6(2-1)^3}\ln x \\
F_8^{(2)}(x) &= \frac{x(3-x)}{4(x-1)^2} - \frac{x}{2(x-1)^3}\ln x
\end{aligned}
$$

Bibliography

[1] K.Nakamura (Particle Data Group), J.Phys.G37,075021 (2010).

[2] A. D. Sakharov, JETP Lett. 5, 24 (1967).

[3] E. W. Kolb and M. S. Turner, Front. Phys. **69**, 1 (1990).

[4] V. A. Kuzmin, V. A. Rubakov and M. E. Shaposhnikov, Phys. Lett. B 155, 36 (1985).

[5] M. E. Shaposhnikov, JETP Lett. 44, 465 (1986) [Pisma Zh. Eksp. Teor. Fiz. 44, 364 (1986)].

[6] M. E. Shaposhnikov, Nucl. Phys. B 287, 757 (1987).

[7] N. S. Manton, Phys. Rev. D 28, 2019 (1983);

[8] F. R. Klinkhamer and N. S. Manton, Phys. Rev. D 30, 2212 (1984).

[9] A. G. Cohen, D. B. Kaplan and A. E. Nelson, Ann. Rev. Nucl. Part. Sci. **43**, 27 (1993) [hep-ph/9302210].

[10] Arnold P, McLerran L, Phys. Rev. D36:581 (1987); Phys. Rev. D37:1020 (1988)

[11] Carson L, Li X, McLerran L, Wang RT, Phys. Rev. D42:2127 (1990)

[12] D. Bodeker, G.D. Moore, and K. Rummukainen, Phys. Rev. D 61, 056003 (2000); G. D. Moore, Phys. Rev. D 62, 085011 (2000).

[13] P. Huet and E. Sather, Phys. Rev. D **51**, 379 (1995) [hep-ph/9404302].

[14] D. E. Morrissey and M. J. Ramsey-Musolf, New J. Phys. **14**, 125003 (2012) [arXiv:1206.2942 [hep-ph]].

[15] G. W. Anderson and L. J. Hall, Phys. Rev. D 45, 2685 (1992)

[16] M. Sher, Phys. Rep. 179, 275 (1989).

[17] A. I. Bochkarev and M. E. Shaposhnikov, Mod. Phys. Lett. A **2**, 991 (1987) [Erratum-ibid. A **4**, 1495 (1989)].

[18] A. G. Cohen, D. B. Kaplan and A. E. Nelson, Ann. Rev. Nucl. Part. Sci. 43, 27 (1993) [hep- ph/9302210].

[19] M. Ahmadvand, Int. J. Mod. Phys. A **29**, 1450090 (2014) [arXiv:1308.3767 [hep-ph]].

[20] J. M. Cline, K. Kainulainen and M. Trott, JHEP **1111**, 089 (2011) [arXiv:1107.3559 [hep-ph]].

[21] V. Cirigliano, Y. Li, S. Profumo and M. J. Ramsey-Musolf, JHEP **1001**, 002 (2010) [arXiv:0910.4589 [hep-ph]].

[22] J. Shu and Y. Zhang, Phys. Rev. Lett. **111**, no. 9, 091801 (2013) [arXiv:1304.0773 [hep-ph]].

[23] J. Engel, M. J. Ramsey-Musolf and U. van Kolck, Prog. Part. Nucl. Phys. **71**, 21 (2013) [arXiv:1303.2371 [nucl-th]].

[24] T. Chupp and M. Ramsey-Musolf, [arXiv:1407.1064 [hep-ph]].

[25] Y. Li, S. Profumo and M. Ramsey-Musolf, Phys. Lett. B **673**, 95 (2009) [arXiv:0811.1987 [hep-ph]].

[26] W. Bernreuther and M. Suzuki, Rev. Mod. Phys. **63**, 313 (1991) [Erratum-ibid. **64**, 633 (1992)].

[27] J. Baron *et al.* [ACME Collaboration], Science **343**, no. 6168, 269 (2014) [arXiv:1310.7534 [physics.atom-ph]].

[28] M. P. Altarelli and F. Teubert, Int. J. Mod. Phys. A **23**, 5117 (2008) [arXiv:0802.1901 [hep-ph]].

[29] G. C. Branco, L. Lavoura and J. P. Silva, Int. Ser. Monogr. Phys. **103**, 1 (1999).

[30] V. Weisskopf and E. Z. Wigner, Z. Phys. 63 (1930) 54; 65 (1930) 18.

[31] T. Liu, M. J. Ramsey-Musolf and J. Shu, Phys. Rev. Lett. **108**, 221301 (2012) [arXiv:1109.4145 [hep-ph]].

[32] J. M. Cline, M. Joyce and K. Kainulainen, J. High Energy Phys. 07 (2000) 018; M. S. Carena, M. Quiro´ s, M. Seco, and C.E.M. Wagnerd, Nucl. Phys. B650, 24 (2003).

[33] P. Huet and A. E. Nelson, Phys. Rev. D 53, 4578 (1996).

[34] A. Megevand and A.D. Sa´nchez, Nucl. Phys. B825, 151 (2010).

[35] A. J. Buras, L. Merlo, and E. Stamou, JHEP 1108 (2011) 124, arXiv:1105.5146 [hep-ph].

[36] S. C. Park, J. Shu, K. Wang, and T. T. Yanagida, Phys. Rev. D 82, 114003 (2010).

[37] A. Lenz and U. Nierste, J. High Energy Phys. 06 (2007) 072.

[38] J. Laiho, E. Lunghi, and R. S. Van de Water, Phys. Rev. D 81, 034503 (2010).

[39] G. W. Anderson and L. J. Hall, Phys. Rev. D 45, 2685 (1992).

[40] R. R. Parwani, Phys. Rev. D 45, 4695 (1992) [Erratum-ibid. D 48, 5965 (1993)] [hep-ph/9204216].

[41] M. E. Carrington, Phys. Rev. D 45, 2933 (1992).

[42] P. B. Arnold and O. Espinosa, Phys. Rev. D 47, 3546 (1993) [Erratum-ibid. D 50, 6662 (1994)] [hep-ph/9212235].

[43] Heavy Flavor Averaging Group Collaboration, Y. Amhis et al., arXiv:1207.1158 [hep-ex].

[44] F. Mahmoudi, "SuperIso v2.3: A Program for calculating flavor physics observables in Supersymmetry," Comput.Phys.Commun. 180 (2009) 1579–1613, arXiv:0808.3144 [hep-ph].

[45] M. Pospelov and A. Ritz, Annals Phys. **318**, 119 (2005) [hep-ph/0504231].

[46] G. C. Branco, P. M. Ferreira, L. Lavoura, M. N. Rebelo, M. Sher and J. P. Silva, Phys. Rept. **516**, 1 (2012) [arXiv:1106.0034 [hep-ph]].

[47] A. Denner, Fortsch. Phys. **41**, 307 (1993) [arXiv:0709.1075 [hep-ph]].

[48] G. D. Moore, Phys.Lett. B412 (1997) 359–370, arXiv:hep-ph/9705248 [hep-ph].

[49] M. Misiak and M. Steinhauser, Nucl.Phys. B764 (2007) 62–82, arXiv:hep-ph/0609241 [hep-ph].

[50] M. Blanke, A. J. Buras, K. Gemmler, and T. Heidsieck, JHEP 1203 (2012) 024, arXiv:1111.5014 [hep-ph].

[51] M. Blanke, B. Shakya, P. Tanedo, and Y. Tsai, JHEP 1208 (2012) 038, arXiv:1203.6650 [hep-ph].

[52] B. Aubert *et al.* [BaBar Collaboration], Phys. Rev. D **79**, 052003 (2009) [arXiv:0809.1174 [hep-ex]].

[53] A. J. Buras, S. Jager and J. Urban, Nucl. Phys. B **605**, 600 (2001) [hep-ph/0102316].

[54] A. Tranberg and B. Wu, JHEP **1207**, 087 (2012) [arXiv:1203.5012 [hep-ph]].

[55] T. Cohen, D. E. Morrissey and A. Pierce, Phys. Rev. D **86**, 013009 (2012) [arXiv:1203.2924 [hep-ph]].

[56] D. Curtin, P. Jaiswal and P. Meade, JHEP **1208**, 005 (2012) [arXiv:1203.2932 [hep-ph]].